International Journal of Engineering Research & Management Technology
(Peer-Reviewed, Open Access, Fully Refereed International Journal) ISSN: 2348-4039
Volume 11, Issue-5, September-October- 2024 Impact Factor: 7.09
Email: editor@ijermt.org www.ijermt.org

ANALYSIS OF TRANSMITTANCE SPECTRA IN 1D PHOTONIC CRYSTAL STRUCTURES WITHIN THE ULTRAVIOLET REGIME

Umesh Kumar
Ph.D. Scholar
Department of Physics
Malwanchal University Indore, (M.P.).

Dr. V. K Suman
Supervisor
Department of Physics
Malwanchal University Indore, (M.P.).

ABSTRACT

Photonic crystals, also known as PhCs, are a type of structured material that possesses photonic band gaps known as wavelength bands in the optical spectrum. These gaps are caused by Bragg diffraction, which causes light to reflect on the periodic structure. The preparation of one-dimensional (1D) PhCs may be accomplished in a manner that is low-cost, scalable, and repeatable by the process of anodizing valve metals under regularly oscillating circumstances. Chemical sensors, low-threshold lasers, optical filters, photonic tags, and photocatalysis are all examples of applications that make use of photocrystals (PhCs) that are based on anodic aluminum oxide (AAO). In this study, we created a one-dimensional semiconductor photonic crystal structure that was composed of two layers of semiconductor material. We then used the transfer matrix approach to investigate the optical characteristics of this structure.

Keyword: semiconductor, PhCs, transfer matrix, Ultraviolet

INTRODUCTION:

Photonic crystals, also known as PhCs, are a distinct category of materials that are periodically organized and possess translational symmetry in one, two, or three dimensions. [1] Over the course of the past three decades and a half, they have garnered a considerable amount of attention due to the fact that they have the potential to effectively regulate and manipulate electromagnetic (EM) waves that are present. "[2–4]" PhCs display a photonic band gap (PBG) whenever the periodicity of the dielectric constant is of the same order of magnitude as the wavelength of the probe light. This is a phenomenon in which the propagation of a certain light wavelength range is partially impeded or even fully disallowed. The photonic bandgap (PBG) is a physical consequence that arises as a result of the many optical reflections that occur at the interfaces of the layers. These reflections give rise to constructive interference, which in turn results in a photonic resonance characteristic when the reflectance is high. Another uniqueness of PhCs is the amplification of the local electromagnetic field, which is directly associated to the abnormal group velocity dispersion at the borders of the PBG6. This dispersion causes a longer interaction time between light and material, which results in a longer interaction time. [7–9] A Due to the fact that they possess these one-of-a-kind characteristics, PhCs have been exploited in a broad variety of applications, either as random porous structures or as self-assembled periodical structures. [10–12] Porous silicon (pSi), which is created by the electrochemical anodization of crystalline silicon (cSi) wafers, has been demonstrated to be an extremely excellent dielectric material for the construction of one-dimensional (1D) PhCs. This is owing to the fact that the etching process is quite straightforward. ages 13–15 The fact that the sections of the pSi PhCs that have previously been etched are unaffected by subsequent etching was the most important insight that led to the successful fabrication of pSi PhCs. Furthermore, the temporal modulation of the etching current causes variations in the porosity of the substrate, which is then linearly related with the refractive index. These changes are the result of the etching current being variable over time. Because of this characteristic, it is possible to vary the porosity-depth profile of pSi, and it is also possible to fabricate any combination of layers with the requisite optical thicknesses. [16] Therefore, the desired optical characteristics of pSi PhCs may be modified to appear in the appropriate spectral area. This is accomplished by adjusting the etching settings and the computer-controlled etch waveform that has been designed.

[17] In the wake of the initial results that Vincent18 and Berger et al.[19] published, several pSi multilayer systems have been experimentally documented and have found widespread use. [20–22] Rugate filters, which feature a continuous, sinusoidally fluctuating distribution of the refractive index in the direction that is perpendicular to the filter plane, have been among the most common optical structures among these. [23]

OBJECTIVE OF THE STUDY

1. The transmittance spectra of incoming light on the suggested structure in the ultraviolet zone should be studied.
2. Designed and analyzed the optical characteristics of a one-dimensional semiconductor photonic crystal structure with two layers of semiconductor material using the transfer matrix method.

REVIEW OF THE LITERATURE

Aouachir et al.(2025) For the purpose of real-time detection of human blood components in the visible wavelength region, the purpose of this work is to explore the transmittance spectrum of a one-dimensional photonic crystal 1D-PhC biosensor that is comprised of SiO2/TiO2 multilayers. Obtaining the transmittance spectrum of the sensor was accomplished through the utilization of the Transfer Matrix Method (TMM) that was built in Python. Within the photonic band gap (PBG) of wavelength between 650 and 1050 nm and 2170 nm thickness of the defect layer, the proposed sensor is able to detect shifts in the transmittance profile of four selected blood compound indices (blood plasma, white blood cells, hemoglobin, and red blood cells) in an efficient manner. This is accomplished by utilizing seven periodic layers of TiO2/SiO2 and a 20° incident theta angle. For the purpose of optimizing the sensor performance, a parametric analysis was carried out by altering the defect layer thickness d0, the number of periodic layers N, and the incidence angle θi. While retaining high sensitivity and quality factors throughout a wide range of concentrations, the improved sensor design was able to detect tiny variations in the refractive index produced by fluctuations in hemoglobin levels. This was accomplished at a time when d0 was equal to 10D and N was equal to 7.

Sagar and Kumar's (2023) In this paper, a Bragg mirror structure was developed with a SiO2 top layer to generate resonance in the ultraviolet (UV) wavelength region. The structural parameters were adjusted to excite a Bloch surface wave with a wavelength of 256 and 281 nm at the top interface, which are the operational wavelengths. This was done in order to generate resonance in the UV wavelength region.

Ferdous, (2023) By altering the design of the one-dimensional photonic crystal (1D-PhC) structure in the suitable manner, this work demonstrates the wavelength at which sensitivity occurs. It is necessary to make adjustments to the structural parameters in order to excite a Bloch surface wave at the top interface, which has a wavelength of 256 and 281 nm. These wavelengths are the operational wavelengths. The distribution of electric fields and mode confinement in the spectrum provided confirmation of the proposed structure, which was found to have a defect layer that was 8 nanometers thick. The design that has been presented is sensitive to changes in the refractive index value of the analyte at visible light wavelengths. According to the findings of the experiment, the sensitivity is approximately 107.42 and 101.85 degrees per radial arm unit (RIU), and the quality factor is 1426.17 and 1708.14 nanometers at UV wavelengths of 281 and 256 nanometers, respectively.

Srivastava's (2014) work There are three MgF2/SrTiO3 MQWs that make up the structure that has been presented. Using the reflectance spectra of the one-dimensional MQW photonic crystal structure that was generated by the Transfer Matrix Method (TMM), an investigation into the range of reflection band is carried out. Based on the numerical analysis, it has been discovered that the range of reflection band for a single MQW PC is quite small, despite the fact that it rises as the thickness of layers increases. Under typical incidence conditions, however, the utilization of three MQWs of MgF2/SrTiO3 results in a significantly larger reflection band that spans the wavelength range of 119.8 nm to 311.3 nm (reflectivity more than 99%) and has a bandwidth of 191.5 nm. Furthermore, we see that as the angle of incidence is raised, the breadth of the reflection band grows in the case of TE waves, while it decreases for TM waves. This is due to the fact that the omnidirectional reflection (ODR) band is extremely small in the ultraviolet area. We have performed computations on the ODR band up to an incidence angle of 50 degrees for both single and coupled MQW PC. When we examine the reflectance curve at incidence angles up to 50 degrees for both TE and TM polarizations, we see that the application of the combined MQW PC

results in a considerable increase in the omnidirectional reflection band when compared to the single MQW structure. The MQW photonic crystal structure that has been presented is extremely helpful in the construction of ultraviolet shielding for pharmaceuticals, ultraviolet reflectors for protecting DNA from damage, and in the treatment of skin illnesses, particularly skin cancer.

(An, 2011) The result demonstrates that because the dielectric constant is a real quantity, there are m narrow-band transmission resonance peaks that occur in the transmission spectrum. These peaks have the ability to accomplish the function of tunable multi-channel optical filtering. With the addition of active matter, there is only one super-narrow-band resonance peak that appears at the normalized center frequency of 1.0ω/ω0. This resonance peak strongly gains with a multiple of up to 104 orders of magnitude. This occurs when the layer C is the complex dielectric constant that contains a negative imaginary part. It is possible to accomplish the functionalities of optical amplifiers and high-performance optical filters. While this is going on, a tremendously powerful stimulated radiation is observed at the normalized center frequency of 1.0π/ω0. A tight relationship exists between the repetition period m and the magnitude of the negative imaginary component of the complex dielectric constant in layer C. This relationship is also present between the transmission gain and the intensities of stimulated radiation. All of these characteristics serve as a theoretical foundation for the work that will be done to prepare for the experiment.

ANALYSIS OF THEORETICAL:

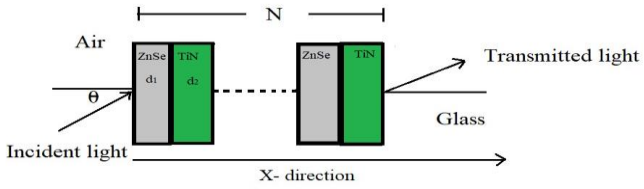


Figure (1): schematic diagram of our one-dimensional photonic crystal structure using ZnSe and TiN for N periods.

The diagram in figure 1 illustrates the geometry of a semiconductor photonic crystal with a single dimension. This structure is made up of two layers that are repeated for N periods at a frequency of N=15. The first layer is made of ZnSe material with a thickness of d1, while the second layer is made of TiN material with a thickness of d2. It has been determined that the refractive index of ZnSe is n1=2.44[25], while the refractive index of TiN is n2=1.56[26]. On the basis of the study of the electric field interaction inside the structure along the given direction in terms of the dynamical and propagating matrices [17, 27], it is possible to derive the interaction that occurs between electromagnetic waves and the current structures.

$$F=\begin{pmatrix} f_{11} & f_{12} \\ f_{21} & f_{22} \end{pmatrix} = D_o{}^{-1}(D_1P_1D_1{}^{-1}D_2P_2D_2{}^{-1})^N D_s \quad (1)$$

$$D_m = \begin{bmatrix} 1 & 1 \\ n_m\cos\theta_m & -n_m\cos\theta_m \end{bmatrix} \quad (2)$$

When m equals zero, one, and two. Within this context, the propagation matrices (P) are expressed as follows:

$$P_{m=}\begin{bmatrix} cos\varphi_l+isin\varphi_l & 0 \\ 0 & cos\varphi_l-isin\varphi_l \end{bmatrix} \quad (3)$$

$$\varphi_l = \frac{2\pi d_l}{\lambda} n_l cos\theta_l \quad (4)$$

Where l=1,2. The matrix elements of equation (3) may be used to get the reflection coefficient:

$$r = \frac{f_{21}}{f_{11}}, R = |r^2| \quad (5)$$

Afterwards, the transmittance may be determined as follows: -

$$T = |t|^2 = \left|\frac{1}{f_{11}}\right|^2 \quad (6)$$

$$A = 1 - (T+R) \quad (7)$$

RESULTS AND DISCUSSION:

We are going to talk about the outcomes of our simulation in this part. One-dimensional semiconductor photonic crystal is seen in figure (1). This type of photonic crystal is made up of two semiconductor materials that are repeated for N periods. The ZnSe material with a refractive index of n1=2.6 and a thickness of d1 makes up the first layer, while the titanium dioxide material with a refractive index of n2=1.288 and a thickness of d2 makes up the second layer. d_2, at $d_1 + d_2 = \lambda/4$ the number of periods of N=15 period, with two-fourths of the substrates on glass, and the usual incidence of light waves$\theta=0^0$. As shown in Figure 2, the transmittance spectrum is plotted against the wavelength at the point where the incident light waves are at their normal incidence. In the ultraviolet (UV) regions, we have found a photonic bandgap (PBG) with a width of 63.8 nm. The right edge of the PBG is located at 260.6 nm, while the left edge is located at 196.8 nm. Due to the Bragg scattering, which creates destructive interference between the incident light waves, there is no transmission of ultraviolet light waves across this region [28]. Additionally, there is no transmission of any other light waves. Following this, we will demonstrate the impact that several factors have on the PBG area in order to regulate and design it.

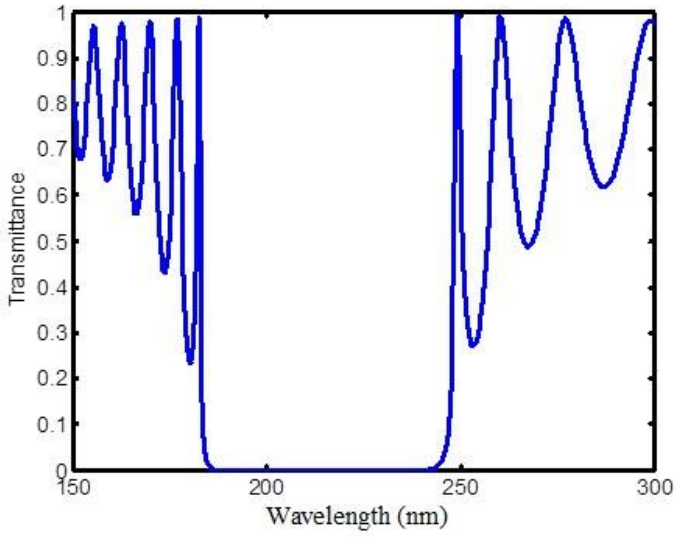


Figure 2: two-material one-dimensional semiconductor photonic crystal transmittance spectra ZnSe, TiN at $\theta = 0^0$

.

The difference in the thickness of the lattice parameter is illustrated in Figure 3, which indicates the effect. $\Lambda = d_1 + d_2$ Figure 3 illustrates the effect by showing the difference in the thickness of the lattice parameter. This difference is representative of the effect.

$$\boldsymbol{d_i} = \left(\frac{1}{n_i}\right)\left(\frac{\lambda_o}{4}\right) \quad (8)$$

Whereas di represents the thickness of the layers, i and ni represent the refractive index of the layers λ_0, and 2 represents the wavelength that is central to the reflection band. If we take the reflectance of such a quarterwave stack and measure it as a function of the wavelength of the light that is shined on it (assuming that the beam is

perpendicular to the surface), we will discover a broad reflectance band that is centered around λ_0. We are able to observe that the photonic bandgap has moved to an area with a higher wavelength, and another two bandgaps that are more acute have appeared.

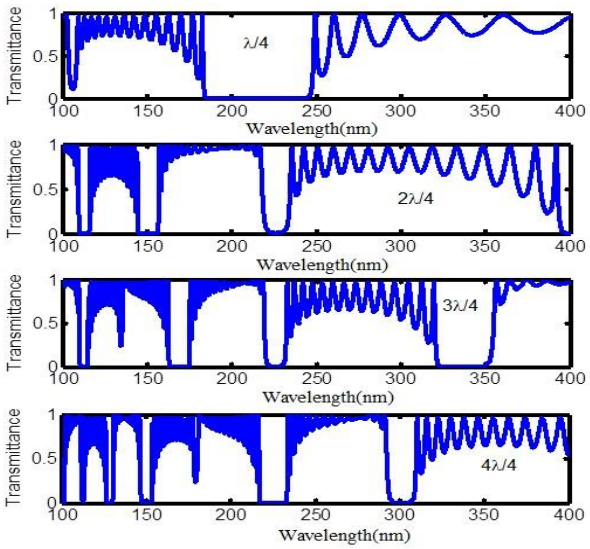


Figure 3: Studying how periodicity thickness affects transmittance.

As can be seen in figure 3, the first bandgap emerged at a wavelength ranging from 220.3 to 231.9 nanometers, the second bandgap occurred at wavelengths ranging from 144.7 to 156.4 nanometers, and the third bandgap covered the range from 109.8 to 115.9 nanometers. When the value of $\Lambda = 3(\lambda/4)$ times the square of four, the width of the band gap rises, and the number of band gaps likewise increases, ultimately reaching four bandgaps in the ultraviolet. At a wavelength of $\Lambda = \lambda$, an additional bandgap emerges in the ultraviolet (UV) region, bringing the total number of band gaps to five. Additionally, the first bandgap relocates to a higher wavelength area. Due to the rise in the width of the bandgap and the introduction of new ones, the thickness of the ZnSe material in our suggested structure is an essential parameter that might block a significant amount of ultraviolet radiation. This is because of the material's ability to impede the transmission of UV radiation.

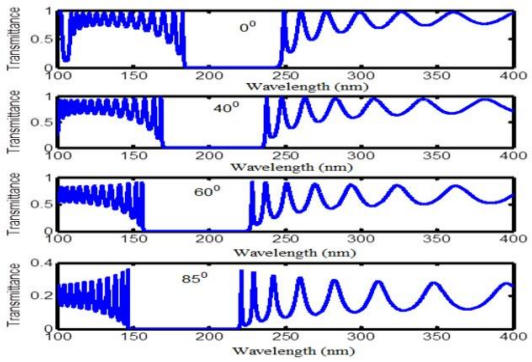


Figure.4: Changing incidence angle transmittance spectra of the proposed structure.

Figure 4 depicts our investigation into the impact that altering the angle of incidence has on the suggested structure as well as the PBG region, which is an essential component in the process of blocking the damaging UV light waves. In order to investigate this impact, we established the thickness of our structure at Λ = lambda/4 and the number of periods at N=15. In the case of the normal incidence, $\theta=0^0$, we are able to see the effect. The width of the bandgap is at 63.8 nm. When the incidence angle is increased to $\theta=40^0$, we observe that the photonic bandgap area shifts to a lower wavelength region, resulting in an increase in its width to 66.3nm. At the value of $\theta = 60^0$, the bandgap

area exhibits a greater shift towards the lower wavelength region, and the breadth increases to 70.3nm. In the end, when the value of $\theta = 85^0$, the width of the bandgap reaches 83.7 nm and shifts farther into a lower wavelength area. Taking into consideration these findings, we are able to assert that the structure that we have presented is advantageous in a number of applications involving optical filters, such as the smart window, because of the width of the photonic bandgap and the capability to adjust it.

CONCLUSION:

Using the transfer matrix approach, we carried out a theoretical investigation on a one-dimensional photonic crystal that was composed of two semiconductor materials, namely ZnSe and TiN. We looked at how the transmittance spectra changed as we changed the characteristics of our structure, such as the thickness and the angle at which the incident light was coming from. An increase in thickness results in an increase in the number of photonic bandgap molecules. The photonic bandgap saw a dramatic change as the incidence angle increased, which was another interesting finding. Furthermore, we are able to confirm that the structure of our proposal plays a significant role in a wide variety of optical applications, including smart windows and optical filters.

REFERENCE

1. Aouachir, A., Benbelgacem, K., Aiadi, K. E., Bentouila, O., & Benrezkallah, A. (2025). Transmittance Spectrum Analysis of a (SiO_2/TiO_2) One-dimensional Defective Photonic Crystal Structure for some Human Blood Compound Sensing. Materials Science-Medziagotyra. https://doi.org/10.5755/j02.ms.41000
2. Sagar, K., & Kumar, A. (2023). Assessment of Bloch surface wave-based one-dimensional photonic crystal sensor using ultraviolet range. Journal of Nanophotonics, 17, 016009. https://doi.org/10.1117/1.JNP.17.016009
3. Ferdous, W. (2023). Assessment of Bloch surface wave-based one-dimensional photonic crystal sensor using ultraviolet range. Journal of Nanophotonics, 17(01). https://doi.org/10.1117/1.jnp.17.016009
4. Srivastava, S. K. (2014). Investigation of Ultra-Wide Reflection Bands in UV Region by Using One-Dimensional Multi Quantum Well Photonic Crystal. Progress in Electromagnetics Research M, 38, 37–44. https://doi.org/10.2528/PIERM14062308
5. An, S. (2011). Transmission spectrum of one-dimensional photonic crystal for realizing high-performance optical transmission function. https://doi.org/10.3969/j.issn.1007-2276.2011.06.022.
6. Yablonovitch E. “Photonic Band-Gap Structures”. J. Opt. Soc. Am. B. 1993. 10(2): 283–295. https://doi.org/10.1364/JOSAB.10.000283
7. Joannopoulos J.D., Villeneuve P.R., Fan S. “Photonic Crystals: Putting a New Twist on Light”. Nature. 1997. 386: 143–149. https://doi.org/10.1038/386143a0
8. Joannopoulos J.D., Johnson S.G., Winn J.N., et al. Photonic Crystals: Molding the Flow of Light. New Jersey: Princeton University Press, 2008.
9. Massaro A. Photonic Crystals: Introduction, Applications, and Theory. Rijeka, Croatia: Intech, 2012. https://doi.org/10.5772/1971
10. Lopez C. “Materials Aspects of Photonic Crystals”. Adv. Mater. 2003. 15(20): 1679–1704. https://doi.org/10.1002/adma.200300386
11. Imhof A., Vos W.L., Sprik R., Lagendijk A. “Large Dispersive Effects Near the Band Edges of Photonic Crystals”. Phys. Rev. Lett. 1999. 83(15): 2942–2943. https://doi.org/10.1103/PhysRevLett.83.2942
12. Mihi A., Míguez H. “Origin of Light-Harvesting Enhancement in Colloidal-Photonic-Crystal-Based Dye-Sensitized Solar Cells”. J. Phys. Chem. B. 2005. 109(33): 15968–15976. https://doi.org/10.1021/jp051828g
13. Gorelik V.S. “Optics of Globular Photonic Crystals”. Laser Phys. 2007. 37: 409–432. https://doi.org/10.1134/S1054660X08120153
14. Dubey R.S., Sarojini P.L. “Light Trapping Mechanism in One-Dimensional (1D) Photonic Crystals for Silicon-Based Solar Cells”. J. Electromagn. Waves Appl. 2013. 27(3): 309–317. https://doi.org/10.1080/09205071.2013.744284

15. Fenzl C., Hirsch T., Wolfbeis O.S. "Photonic Crystals for Chemical Sensing and Biosensing". Angew. Chem., Int. Ed. 2014. 53(13): 3318–3335. https://doi.org/10.1002/anie.201307828
16. Priolo F., Gregorkiewicz T., Galli M., Krauss T.F. "Silicon Nanostructures for Photonics and Photovoltaics". Nature Nanotechnol. 2014. 9(1): 19–32. https://doi.org/10.1038/nnano.2013.271
17. Aly, A. H., Ryu, S.W., Hsu, H.T., & Wu , A.J. (2009). THz transmittance in one-dimensional superconducting nanomaterial-dielectric superlattice. Materials Chemistry and Physics 113, 382-384.
18. Kuznetsov A.I., Miroshnichenko A.E., Brongersma M.I., et al. "Optically Resonant Dielectric Nanostructures". Science. 2016. 354(3614): aag2472. https://doi.org/10.1126/science.aag2472
19. Pavesi L. "Porous Silicon Dielectric Multilayers and Microcavities". Riv. Nuovo Cim. 1997. 20: 1–76. https://doi.org/10.1007/bf02877374
20. Birner A., Wehrspohn R.B., Gösele U.M., et al. "Silicon-Based Photonic Crystals". Adv. Mater. 2001. 13(6): 377–388. https://doi.org/10.1002/1521-4095(200103)13%3A6<377%3A%3AAID-ADMA377>3.0.CO%3B2-X.
21. Estevez J.O., Agarwal V. "Porous Silicon Photonic Crystals". In: Canham L., editor. Handbook of Porous Silicon. Cham: Springer International Publishing, 2014. Pp. 805–814. https://doi.org/10.1007/978-3-319-05744-6_82
22. Agarwal V. "Porous Silicon Multilayers and Superlattices". In: Canham L., editor. Handbook of Porous Silicon. Cham: Springer International Publishing, 2014. Pp. 153–162.
23. Sailor M.J. "Porous Silicon in Practice. Preparation, Characterization and Applications". In: Sailor M.J., editor. Preparation of Micro-, Meso-, and Macro-Porous Silicon. Weinheim, Germany: Wiley-VCH, 2012. Chap. 2, Pp. 52–55. https://doi.org/10.1002/9783527641901.ch2
24. Vincent G. "Optical Properties of Porous Silicon Superlattices". Appl. Phys. Lett. 1994. 64: 2367–2369. https://doi.org/10.1063/1.111982
25. www.Refractiveindex.Info
26. www.filmetrics.com
27. Yeh, P. (1988). Optical Waves in Layered Media. Wiley, New York.
28. Mulder, H.K., Ymeti,A., Subramaniam,V., Kanger,J.S. (2012). Size-selective detection in integrated optical interferometric biosensors .Opt Express, 20,20934–20950.
29. Berger M.G., Arens-Fischer R., Thönissen M., Krüger M., et al. "Dielectric Filters Made of PS: Advanced Performance by Oxidation and New Layer Structures". Thin Solid Films. 1997. 297(1–2): 237–240. https://doi.org/10.1016/S0040-6090(96)09361-3
30. Pacholski C. "Photonic Crystal Sensors Based on Porous Silicon". Sensors. 2013. 13(4): 4694–4713. https://doi.org/10.3390/s130404694
31. Harraz F.A. "Porous Silicon Chemical Sensors and Biosensors: A Review". Sens. Actuators B. 2014. 202: 897–912. https://doi.org/10.1016/j.snb.2014.06.048
32. Vendamani V.S., Rao S.V.S.N., Pathak A.P., Soma V.R. "Silicon Nanostructures for Molecular Sensing: A Review". ACS Appl. Nano. Mater. 2022. 5(4): 4550–4582. https://doi.org/10.1021/acsanm.1c04569
33. Bovard B.G. "Rugate Filter Theory: An Overview". Appl. Opt. 1993. 32(28): 5427–5442. https://doi.org/10.1364/AO.32.005427